Phase Diagram of the Excitonic Insulator

B. Hülsen[1,2], F. X. Bronold[2], H. Fehske[2], and K. Yonemitsu[3]

[1]Fritz-Haber-Institut Berlin [2]Institut für Physik, Universität Greifswald [3]Institute for Molecular Science, Okazaki

Abstract

Motivated by recent experiments, which give strong evidence for an excitonic insulating phase in $TmSe_{0.45}Te_{0.55}$, we developed a scheme to quantitatively construct, for generic two-band models, the phase diagram of an excitonic insulator. As a first application of our approach, we calculated the phase diagram for an effective mass two-band model with long-range Coulomb interaction. The shielded potential approximation is used to derive a generalized gap equation controlling for positive (negative) energy gaps the transition from a semi-conducting (semi-metallic) phase to an insulating phase. Numerical results, obtained within the quasi-static approximation, show a steeple-like phase diagram in contrast to long-standing expectations.

Motivation

The possibility of an excitonic insulator (EI) phase, separating, below a critical temperature, a semiconducting from a semi-metallic phase, has been predicted by theorists more than three decades ago [1]. However, experimental efforts to establish this phase in actual materials largely failed. It is only until recently, that detailed experimental investigations of $TmSe_{0.45}Te_{0.55}$ suggested the existence of an EI phase in this compound [2, 3]. The pressure dependence of the electrical resistivity below $270K$, for instance, strongly points towards an emerging EI phase [2]. Further evidence for collective behavior which may have its origin in an EI phase comes from the linear increase of the thermal conductance and diffusivity at very low temperatures [3].

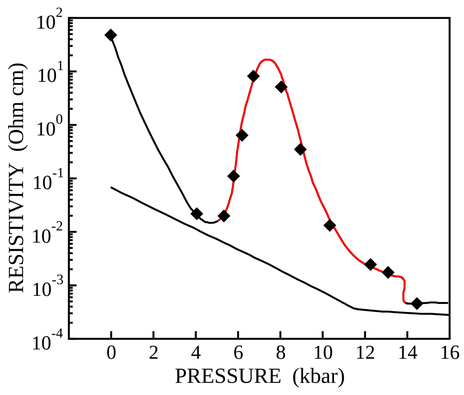

Fig 1: Pressure dependence of the electrical resistivity of $TeSe_{0.45}Te_{0.55}$ for T=4.2K (upper curve) and T=300K (lower curve). Data from Ref. [2].

Under the assumption that the external pressure controls the energy gap E_g, the resistivity data have been used to construct a phase diagram for $TmSe_{0.45}Te_{0.55}$ in the E_g-T plane [2]. Although experimental data strongly suggest that this phase diagram is the phase diagram of an EI, to unambiguously decide if this interpretation is correct requires further theoretical examination.

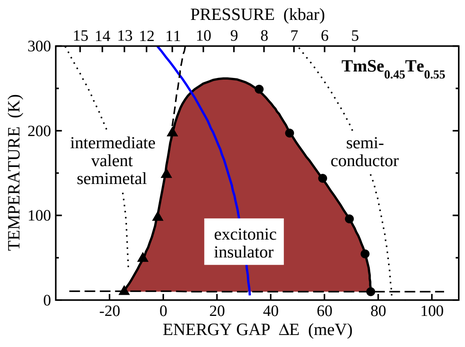

Fig 2: Phase diagram for $TeSe_{0.45}Te_{0.55}$ as obtained from the resistivity data [3].

Model

A *quantitative* phase diagram for an EI has never been calculated, even not for the simplest two-band model: an isotropic, effective mass two-band model for (spinless) valence and conduction band electrons interacting via long-range Coulomb forces.

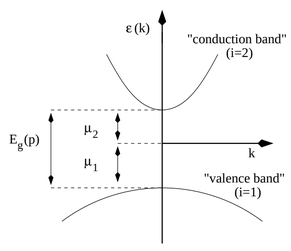

Fig 3: Schematic band structure for an isotropic, effective mass two-band model. Defining momenta $\mathbf{k}_i$ (i=1,2) with respect to the band extrema, the model also holds for an indirect (Γ-X) energy gap.

As a first step towards a theoretical scrutiny of the phases of the $Tm[Se, Te]$ system we present here such a calculation. As far as the actual material is concerned, the model is of course rather crude, neglecting, for instance, strong intraband correlations (due to the mixed valence) and electron-phonon interactions. The two bands should be therefore considered as *effective single-particle bands* describing the electronic degrees responsible for the formation of an EI. With the proper parametrization/interpretation, we expect our results to be also relevant for the Tm[Se,Te] system.

The indirect (Γ-X) energy gap E_g of $Tm[Se, Te]$ can be formally turned into a direct gap by measuring the momenta for conduction (valence) band electrons from the X-point (Γ-point). The Hamiltonian can then be written as

$$H = \sum_i \sum_{\mathbf{k}} \epsilon_i(\mathbf{k}) c^\dagger_{i,\mathbf{k}} c_{i,\mathbf{k}} + \frac{1}{2} \sum_{\mathbf{q}} V_0(\mathbf{q}) \rho(\mathbf{q}) \rho(-\mathbf{q}), \quad (1)$$

with $\rho(\mathbf{q}) = \sum_{i,\mathbf{k}} c^\dagger_{i,\mathbf{k}+\mathbf{q}} c_{i,\mathbf{k}}$ the total charge density and $V_0(\mathbf{q}) = 4\pi e^2/\varepsilon_0 q^2$ the bare Coulomb potential. The dispersions of the two bands are given by ($\hbar = 1$)

$$\epsilon_1(\mathbf{k}) = -\frac{\mathbf{k}^2}{2m_1} + \mu_1, \quad \epsilon_2(\mathbf{k}) = \frac{\mathbf{k}^2}{2m_2} - \mu_2, \quad (2)$$

where μ_1 and μ_2 are the chemical potentials for valence band *holes* and conduction band *electrons*, respectively. If the non-interacting system is an instrinsic semi-conductor ($E_g > 0$),

$$\mu_1, \mu_2 < 0 \text{ and } -\mu_1 - \mu_2 = E_g, \quad (3)$$

whereas for a semi-metal ($E_g < 0$)

$$\mu_1, \mu_2 > 0 \text{ and } \mu_1 + \mu_2 = -E_g = |E_g|. \quad (4)$$

Method

In close analogy to the strong-coupling theory of superconductivity, we employ a matrix propagator formalism. Within the two-band model, the anomalous or off-diagonal (in the band indices $i = 1, 2$) self-energy $\Sigma_{12}(\mathbf{k}, i\omega_n)$ describing the pairing between conduction and valence band electrons, serves as an order parameter: $\Sigma_{12}(\mathbf{k}, i\omega_n) \neq 0$ signals the existence of the EI phase. The order-parameter has to be calculated within a selfconsistent approximation resulting in a nonlinear functional equation whose particular form depends on the physical processes included. Linearizing this equation in the vicinity of the phase boundary, where $\Sigma_{12}(\mathbf{k}, i\omega_n)$ is small, yields, after a quasi-particle approximation, a generalized "gap equation". The phase boundary T(E_g) can then be found by mapping out the T-E_g range for which the "gap equation" has nontrivial solutions.

Shielded potential approximation

To illustrate our selfconsistent approach, we calculate $\Sigma_{12}(\mathbf{k}, i\omega_n)$ within the shielded potential approximation. In terms of diagrams:

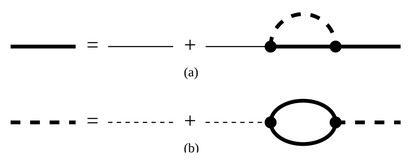

Fig 4: a) Dyson equation for the matrix propagator in the shielded potential approximation. b) Random phase approximation (RPA) for the shielded potential. Thick and thin solid (dashed) lines depict, respectively, dressed and bare matrix propagators (Coulomb interactions).

On the real energy axis, the anomalous self-energy is after linearization given by

$$\begin{pmatrix} \mathrm{Re}\Sigma^r_{12}(\mathbf{k},\omega) \\ \mathrm{Im}\Sigma^r_{12}(\mathbf{k},\omega) \end{pmatrix} = \int \frac{d\omega' d\mathbf{k}'}{8\pi^3} \begin{pmatrix} K_{11} & K_{12} \\ K_{21} & K_{22} \end{pmatrix} \begin{pmatrix} \mathrm{Re}\Sigma^r_{12}(\mathbf{k}',\omega') \\ \mathrm{Im}\Sigma^r_{12}(\mathbf{k}',\omega') \end{pmatrix} \quad (5)$$

with

$$K_{11} = A\ \mathrm{Im}\{G^r_{11}G^r_{22}\} \quad K_{12} = A\ \mathrm{Re}\{G^r_{11}G^r_{22}\} \quad (6)$$
$$K_{21} = B\ \mathrm{Im}\{G^r_{11}G^r_{22}\} \quad K_{22} = B\ \mathrm{Re}\{G^r_{11}G^r_{22}\} \quad (7)$$

and

$$A = V_0(\mathbf{k}-\mathbf{k}')n_F(\omega') + \mathrm{P}\int \frac{d\epsilon}{\pi} \frac{\mathrm{Im}V^r_s(\mathbf{k}-\mathbf{k}',\epsilon)}{\omega'-\omega+\epsilon}[n_F(\omega') + n_B(-\epsilon)] \quad (8)$$
$$B = \mathrm{Im}V^r_s(\mathbf{k}-\mathbf{k}',\omega-\omega')[n_F(\omega') + n_B(\omega'-\omega)]. \quad (9)$$

To simplify Eq. (5), we employ a quasi-particle approximation for the intraband propagators,

$$G^r_{ii}(\mathbf{k},\omega) = \frac{1}{\omega + i\delta - e_i(\mathbf{k}) + i\gamma_i(\mathbf{k})}, \quad (10)$$

with renormalized band dispersions and lifetimes given by

$$e_i(\mathbf{k}) = \epsilon_i(\mathbf{k}) + \mathrm{Re}\Sigma^r_{ii}(\mathbf{k}, e_i(\mathbf{k}))\ , \quad (11)$$
$$\gamma_i(\mathbf{k}) = -\mathrm{Im}\Sigma^r_{ii}(\mathbf{k}, e_i(\mathbf{k})), \quad (12)$$

respectively. Extended calculations have shown, that, within the shielded potential approximation, $e_i(\mathbf{k}) = \epsilon(\mathbf{k}) + \Delta\epsilon$ [4]. The renormalization leads therefore only to a $\mathbf{k}$-independent energy shift which can be included in the definition of the chemical potentials μ_i.

Generalized gap equation

Inserting (10) in (5) and ignoring lifetime effects, that is, setting $\mathrm{Im}\Sigma_{ij} = 0$ for all i and j, we obtain two coupled integral equations for $\mathrm{Re}\Sigma_{12}(\mathbf{k}, e_i(\mathbf{k})) \equiv \Delta_i(\mathbf{k})$, i=1,2. For an isotropic system, $\Delta_i(\mathbf{k}) = \Delta_i(k)$. Instead of k, we use $\epsilon = e_2(k)$ as an integration variable and write the generalized gap equation as follows (measuring energies and length in excitonic Rydbergs and Bohr radii)

$$\Delta_i(\epsilon) = \sum_j \int_{-\mu_2}^{\infty} d\epsilon' U_{ij}(\epsilon,\epsilon')(-)^{1+j} B(\epsilon')\Delta_j(\epsilon'), \quad (13)$$

with $B(\epsilon') = 1/(e'_2 - e'_1)$, $e'_1 = -\alpha(e'_2 + \mu_2) + \mu_1$, $e_2 = \epsilon$, and the mass ratio $\alpha = m_2/m_1$.

Note, in contrast to the gap equation for superconductivity, Eq. (13) is not restricted to the Fermi surface. Instead we keep the full momentum and (on-shell) energy dependence. This is particularly important for low densities, below the Mott density, where bound states (excitons) exist.

Interaction kernel

The interaction kernel depends on the dielectric function $\varepsilon(\mathbf{q}, z)$ which has to be calculated in some approximation. For simplicity we consider a RPA inspired plasmon-pole approximation although this might not be a good approximation at intermediate densities corresponding to small band gaps/overlaps. The dynamically screened Coulomb interaction is then given by

$$V_s(\mathrm{q}, z) = \frac{V_0(\mathrm{q})}{\varepsilon(\mathrm{q}, z)}\ , \quad \varepsilon(\mathrm{q}, z) = 1 + \frac{\omega^2_{pl}}{z^2 - \omega(\mathrm{q})^2}, \quad (14)$$

with $\omega(\mathrm{q}) = \omega_{pl}\sqrt{1 + q^2/\kappa^2}$. The screening wavenumber κ and the plasmon energy ω_{pl} are given below.

Within the plasmon-pole approximation the interaction kernel becomes

$$U^{PPA}_{ij}(\epsilon,\epsilon') = U^x_{ij}(\epsilon,\epsilon') + U^c_{ij}(\epsilon,\epsilon') \quad (15)$$
$$U^x_{ij}(\epsilon,\epsilon') = \frac{1}{\pi k}\log\Big(\frac{k+k'}{k-k'}\Big)^2 n_F(e'_j) \quad (16)$$
$$U^c_{ij}(\epsilon,\epsilon') = \frac{1}{\pi k}\int_{\omega_-}^{\omega_+} d\omega \frac{\omega^2_{pl}}{\omega^2 - \omega^2_{pl}} h(\omega, e_i, e'_j) \quad (17)$$

with

$$h(\omega, e_i, e'_j) = -\frac{n_F(e'_j) + n_B(\omega)}{\omega + e_i - e'_j} + \frac{1 - n_F(e'_j) + n_B(\omega)}{\omega - e_i - e'_j} \quad (18)$$
$$\omega_+ = \omega_{pl}\sqrt{1 + \frac{(k+k')^2}{\kappa^2}} \quad \omega_- = \omega_{pl}\sqrt{1 + \frac{(k-k')^2}{\kappa^2}}. \quad (19)$$

Instead of splitting the interaction kernel into an exchange (U^x_{ii}) and a correlation term (U^c_{ii}), we can alternatively speparate the kernel into a statically screened exchange term (U^{ssx}_{ii}) and a dynamical term (U^{dyn}_{ii}) which accounts for finite recoil energies $e_i - e'_j$. Explicitly:

$$U^{PPA}_{ij}(\epsilon,\epsilon') = U^{ssx}_{ij}(\epsilon,\epsilon') + U^{dyn}_{ij}(\epsilon,\epsilon') \quad (20)$$

with

$$U^{ssx}_{ij}(\epsilon,\epsilon') = V_s(\epsilon,\epsilon')n_F(e'_j) + C(\epsilon,\epsilon') \quad (21)$$
$$V_s(\epsilon,\epsilon') = \frac{1}{\pi k}\log\Big[\frac{(k+k')^2 + \kappa^2}{(k-k')^2 + \kappa^2}\Big] n_F(e'_j) \quad (22)$$
$$C(\epsilon,\epsilon') = \frac{1}{\pi k}\int_{\omega_-}^{\omega_+} d\omega \frac{\omega^2_{pl}}{\omega(\omega^2 - \omega^2_{pl})} \quad (23)$$

and

$$U^{dyn}_{ij}(\epsilon,\epsilon') = \frac{2}{\pi k}\int_{\omega_-}^{\omega_+} d\omega \frac{\omega^2_{pl}}{\omega(\omega^2 - \omega^2_{pl})}\tilde{h}(\omega, e_i, e'_j) \quad (24)$$
$$\tilde{h}(\omega, e_i, e'_j) = f(\omega, e_i, e'_j)n_F(e'_j) + g(\omega, e_i, e'_j) \quad (25)$$
$$f(\omega, e_i, e'_j) = 1 - \frac{\omega}{2}\Big(\frac{1}{\omega + e_i - e'_j} + \frac{1}{\omega - e_i + e'_j}\Big) \quad (26)$$
$$g(\omega, e_i, e'_j) = \frac{\omega}{2}\Big(\frac{1 + n_B(\omega)}{\omega - e_i + e'_j} - \frac{n_B(\omega)}{\omega + e_i - e'_j}\Big) - \frac{1}{2}. \quad (27)$$

Quasi-static approximation

The full analysis of Eq. (13) is the subject of a forthcoming work [5]. Here, we focus on the quasi-static approximation, which neglects the recoil energies $e_i - e'_j$. In that limit U^{dyn}_{ij} vanishes. As a result, $\Delta_1(\epsilon) = \Delta_2(\epsilon) \equiv \Delta(\epsilon)$ and the gap equation reduces to

$$\Delta(\epsilon) = \int_{-\mu_2}^{\infty} d\epsilon' V_s(\epsilon,\epsilon')\frac{n_F(e'_1) - n_F(e'_2)}{e'_2 - e'_1}\Delta(\epsilon'). \quad (28)$$

To obtain a closed set of equations, the chemical potentials have to be determined as a function of temperature and energy gap. Combining the constraint $-\mu_1 - \mu_2 = E_g$, which is just the definition of the energy gap E_g, with particle conservation $n_1 = n_2$, where n_1 is the number of *holes* in the valence band and n_2 the number of *electrons* in the conduction band, we find

$$\int_{-\mu_1}^{\infty} d\epsilon \sqrt{\epsilon + \mu_1} n_F(\epsilon) = \alpha^{\frac{3}{2}} \int_{\mu_1 + E_g}^{\infty} d\epsilon \sqrt{\epsilon - E_g - \mu_1} n_F(\epsilon) \quad (29)$$

from which we determine μ_1. Note, on the semiconducting side, condition (29) takes thermally excited electron-hole pairs into account. The screening wave number follows from

$$\kappa^2 = \frac{\sqrt{2}}{\pi}\Big[\int_{\mu_1+E_g}^{\infty} d\epsilon \frac{n_F(\epsilon)}{\sqrt{\epsilon - E_g - \mu_1}} + \alpha^{-\frac{3}{2}} \int_{-\mu_1}^{\infty} d\epsilon \frac{n_F(\epsilon)}{\sqrt{\epsilon + \mu_1}}\Big] \quad (30)$$

Results

To construct the phase boundary T(E_g), we discretize Eq. (28) and determine, for fixed E_g, the temperature T for which the determinant of the coefficient matrix of the resulting system of linear equations vanishes. For $E_g < 0$ this approach can be directly applied, whereas for $E_g > 0$, the logarithmic singularity of the kernel at $\epsilon = \epsilon'$ has to be removed first [5]. Recall that we measure energies and temperatures in units of the exciton Rydberg R_0.

Here we present results for equal band masses, $m_1 = m_2$, i.e., $\alpha = 1$. In that case, condition (29) pins the chemical potential for all temperatures to the middle of the energy gap/overlap. Thus, $\mu_1 = -\frac{E_g}{2}$ for $E_g > 0$ and $\mu_1 = +\frac{|E_g|}{2}$ for $E_g < 0$.

First we show in Fig. 5 the phase boundary $T(E_g)$ as obtained from Eq. (28) but with temperature independent screening, that is, for $\kappa^2 = \kappa^2(T = 0, E_g)$. A very pronounced steeple-like phase boundary arises. The inset shows $T(E_g)$ for $-E_g \ll T$, where it approaches the asymptotic result $T \approx (\gamma|E_g|/\pi)\exp(-\pi\sqrt{|E_g|}/\ln(1 + \pi\sqrt{|E_g|}/2))$, with $\gamma = \exp(0.577)$ (dashed line in the inset).

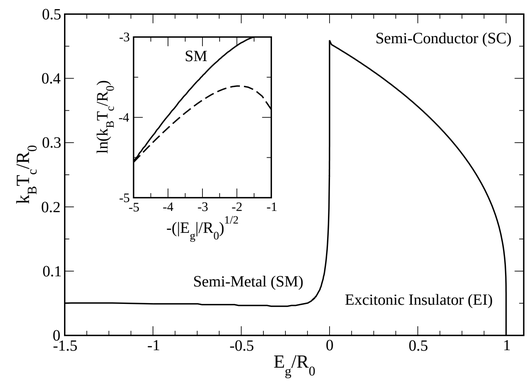

Fig 5: Phase diagram for an excitonic insulator with equal band masses and temperature independent screening.

The temperature dependence of κ^2 is shown in the inset of Fig. 6 for various band gaps/overlaps. For $E_g < 0$, κ^2 is rather large and quickly exceeds the critical screening length given by the Mott criterium $\kappa^2 = 0.71$ above which excitons are unstable. Note, because of thermally excited electron-hole pairs, κ^2 is also finite for $E_g > 0$ and $T > 0$. For small band gaps thermally excited carriers contribute significantly to screening.

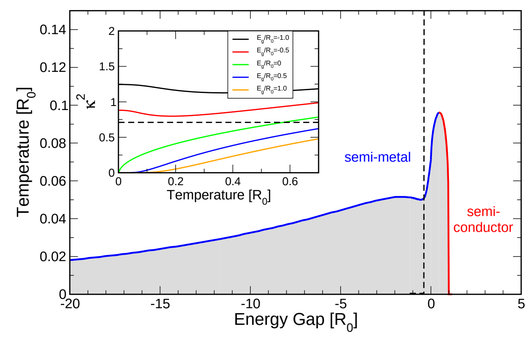

Fig 6: Phase diagram for an excitonic insulator with equal band masses and temperature dependent screening. The dashed line indicates the Mott criterium κ^2=0.71. To the left of this line, (preformed) bound states are unstable. The inset shows κ^2 as a function of temperature for various energy gaps/overlaps.

The phase boundary $T(E_g)$ with temperature dependent screening included is presented in the main panel of Fig. 6. Above $T_1 \approx 0.1$, the EI phase is always unstable. Below T_1, we still find a steeple-like phase boundary which strongly discriminates between $E_g < E^{Mott}_{crit}$ and $E_g > E^{Mott}_{crit}$, with $E^{Mott}_{crit} \approx -0.3$, the critical band overlap for which the Mott criterium is satisfied at T=0. For $E_g > -E^{Mott}_{crit}$, $T(E_g)$ increases very fast, within a few percent of R_0, to a maximum from which it smoothly decreases to zero at $E_g = 1$, the critical band gap, above which the EI phase cannot exist. For $E_g < -E^{Mott}_{crit}$, in contrast, $T(E_g)$ decreases smoothly (after a small initial increase).

The steeple-like shape of the phase diagram reflects the different phases from which the EI is approached: semi-conducting for $E_g > 0$ and semi-metallic for $E_g < 0$. Entering the EI phase from the semi-conductor side always leads to formation of *strongly bound excitons*. On the other hand, when the EI phase is approached from the semi-metal, exciton formation can only occur for $E^{Mott}_{crit} < E_g < 0$; for larger band overlap it is suppressed due to the free carrier's screening of the Coulomb potential. In that case, the "excitonic insulator" is supported by *loosely bound Cooper-type pairs*. As a result the collective phase becomes more fragile. Anisotropies in the band structure and other pair breaking effects would easily destroy this part of the phase diagram [6]. The crossover from excitons to Cooper-type pairs occurs in our calculation at $E_g \approx -0.3$. The precise value of the critical band overlap depends on the screening model. A more realistic treatment of screening, in particular at intermediate densities, is clearly desirable.

Conclusions

Based on an isotropic, effective mass two-band model, we calculated the phase diagram of an excitonic insulator taking screening explicitly into account. We obtain a steeple-like phase boundary which we interpret in terms of a cross-over from preformed excitons at $-0.3 = E^{Mott}_{crit} < E_g < 1$ and Cooper-type electron-hole pairs for $E_g < E^{Mott}_{crit}$. "Excitons" per se support the EI phase therefore only for $-0.3 = E^{Mott}_{crit} < E_g < 1$. To explore the consequences of the cross-over in more detail, in particular in view of the experimentally found phases in the Tm[Se,Te] system, is the subject of on-going research.

Support from SFB 652 is greatly acknowledged.

References

[1] For a review of the early literature, see, e.g. , B. I. Halperin and T. M. Rice, Solid State Physics **21** (1968) 115.

[2] J. Neuenschwander and P. Wachter, Phys. Rev. B **41** (1990) 12693.

[3] P. Wachter, B. Bucher, and J. Malar, Phys. Rev. B **69** (2004) 094502.

[4] H. Haug and S. Schmitt-Rink, Prog. Quantum Electr. **9** (1984) 3.

[5] F. X. Bronold, B. Hülsen, and H. Fehske, in preparation.

[6] J. Zittartz, Phys. Rev. **162** (1967) 752.